

HARDWARE-IN-LOOP SIMULATION AND IMPLEMENTATION OF FUZZY SLIDING MODE CONTROL OF INDUCTION MOTOR BASED ON FPGA

R. SENTHIL KUMAR¹ AND V. GANAPATHY²

¹Department of Electrical Engineering

²Department of Information Technology
SRM University

Kattankulathur, Chennai 603203, Tamil Nadu, India
{senthil.papers; dr.vgee}@gmail.com

Received April 2015; revised October 2015

ABSTRACT. *Hardware implementation suggested in this paper, is a low cost hardware-in-loop structure of fuzzy sliding mode controller (FSMC), for vector controlled induction motor. The use of FPGA, results in a better dynamic response. The work makes use of the hardware-in-loop (HIL) structure of MATLAB to provide a real time controller interface for investigation of FSMC. The scheme was tested on a 3 H.P motor by prototype model, and on a 30 H.P machine through MATLAB/SIMULINK simulation. Various operating conditions were investigated and results prove that the controller is robust and the chattering problem is solved.*

Keywords: Speed control, Field oriented control, Sliding mode control, Induction motor, CPLD

1. **Introduction.** In the past sixty years speed control of induction motors (IM) has been achieved by various control strategies, among which two popular methods are field-oriented control (FOC) and direct torque control (DTC). Both methods decouple the interaction between flux and torque control, and provide good torque response in steady state and transient operation conditions. The major disadvantage in these methods is the hardware implementation, which necessitates high speed processors. Present day electric drives impose fully integrated controllers, which provide several control function in the same device, i.e., control and protection. DSP processors are generally preferred for control applications of this sort; perhaps their applications are limited due to high cost.

IM is the most favored machine for industrial drives due to its simple, robust structure, easy maintenance and reliability. Since IM control with power electronic converters results in a multivariable control plant with high levels of non-linearity, developing a low cost standard design has been a challenging task. Prior researchers have recommended various speed control methods for IM like synchronous control [1], slip control [2], flux control and V/F control [3-6] and field oriented control [7-17]. Sliding mode controller (SMC) is one of the effectual methods for controlling electric drive system. It is a robust control, as the high-gain feedback control input eliminates nonlinearities owing to parameter variations and external disturbance. It also offers a fast dynamic response and enhanced stability [18-21]. Sliding mode control has been opted for applications like robot manipulators and tracking control systems. The disadvantage of sliding mode control is that sudden large changes in process variable create high stress on the system, which leads to chattering effect. To avoid these demerits, the traditional sliding mode was replaced by a fuzzy

sliding mode control (FSMC) in this research. The practical application of this FSMC is listed below.

1. Energy conservation mode is required in recent drive units, where the acceleration current is kept low during rise in speed. The smooth transition of speed can be achieved by SMC.
2. Yet another practical application of this vector control drive is the treadmill used in physical fitness centers. This application required the A.C motor to operate at different speed and torque levels to suit various strength levels of runners. Further this application requires the machine to function with stable output at low speeds also; this could be achieved by using an FSMC.

2. Mathematical Model of FSMC. The differential equations of the motor are expressed in the synchronously rotating (d - q) reference frame by transformations, with stator current and rotor flux components as state variables. The drive is modeled into two linear decoupled subsystems, as similar that of a D.C motor [13]. In obtaining the mathematical model of the IM the following assumptions are made.

1. The stator winding is distributed so as to generate a pure sinusoidal MMF in the air gap. The current and voltage harmonics are to be neglected.
2. The slots present in stator and rotor produce no variation in respective inductance and mutual inductances (i.e., are equally distributed)
3. Magnetic saturation effect, Hysteresis, Skin effect and Eddy Current losses are neglected.

Modeling of the vector controlled drive is divided into headings and discussed in this section. The three-phase voltages, currents and fluxes of AC-motors can be analyzed in terms of the space vector which can be defined as follows. Assuming that i_a , i_b and i_c are the instantaneous currents in the stator phases, then the stator current vector i_s (Figure 1) is defined by,

$$\vec{i}_s = \frac{2}{3} (i_a + \alpha i_b + \alpha^2 i_c) \quad (1)$$

where, i_a , i_b and i_c are stator currents in the stationary frame.

This approach in vector control of induction machine modeling was projected in literature during 1980's (like the d - q components by Takahashi; α - β components by Depenbrock; generalized d - q components by De Donker). The stator current space vector i_s depicts the three phase sinusoidal system which needs to be transformed into a two time invariant co-ordinate system. This transformation can be split into two steps.

2.1. Clarke and Park transformations. Three phase stationary quantities (a, b, c) to (α, β) two phase stationary conversion is done using the Clarke transformation (Figure 2). Here the outputs are in a two co-ordinate time variant. A mathematical solution of these time varying quantities is difficult.

$$i_{s\alpha} = i_a \quad (2)$$

$$i_{s\beta} = -i_a \frac{1}{\sqrt{3}} + \frac{3}{\sqrt{3}} i_b \quad (3)$$

Two phase stationary (α, β) to Two phase rotating (d, q) conversion is done using the Park transformation (Figure 3) which outputs a two co-ordinate time invariant system. Here it is notable that the d - q reference frame is rotating in nature. The relation between the two reference frames is given by,

$$i_{sd} = i_{s\alpha} \cos \theta + i_{s\beta} \sin \theta \quad (4)$$

$$i_{sq} = -i_{s\alpha} \sin \theta + i_{s\beta} \cos \theta \quad (5)$$

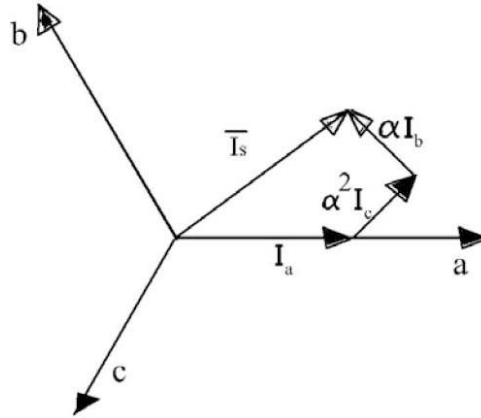


FIGURE 1. Space vectors for stator current

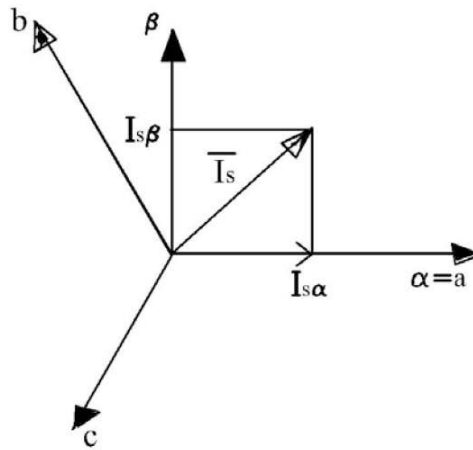


FIGURE 2. Clarke transformation

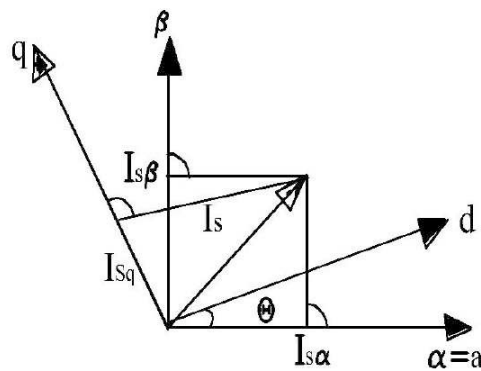


FIGURE 3. Park transformation

In this rotating frame the variables used are time invariant in nature (proposed by Robeter H. Park). Such a time invariant system can be very useful in control application as the complexity of the differential equation has been reduced due to time invariance. The same transformations apply for flux linkages and phase voltages. For a magnetically

linear machine, the stator and rotor flux linkages are given by,

$$\begin{bmatrix} \vec{\lambda}_s \\ \vec{i}_r \end{bmatrix} = \begin{bmatrix} L_s & L_m \\ L_m & L_s \end{bmatrix} \begin{bmatrix} \vec{i}_s \\ \vec{i}_r \end{bmatrix} \tag{6}$$

Normally the IM is of squirrel cage type and then in such a case the rotor is not available for control. Then in such case we can transform the rotor variables into the stator reference frame using Equation (7).

$$\begin{bmatrix} \vec{\lambda}_r \\ \vec{i}_r \end{bmatrix} = e^{j\beta} \begin{bmatrix} n \\ 1/n \end{bmatrix} \begin{bmatrix} \lambda'_r \\ i'_r \end{bmatrix} \tag{7}$$

where, $\beta \dots \dots \dots j\omega dt$, $\omega \dots \dots \dots$ angular speed in rad/s.

2.2. Speed controller. The speed measured using quadrature encoder W_r is compared with the reference speed (W_r^*) and the resulting error (positive or negative) is processed through the speed controller. The speed error at the n^{th} sampling instant is expressed as,

$$W_{e(n)} = W_r^* - W_r \tag{8}$$

Prior researchers have proposed speed controllers based on PI, PID, fuzzy and sliding mode. In this work the FSMC is proposed to take the combined advantage of fuzzy and sliding mode controllers.

2.3. Induction motor. The IM is the main working horse (runs at the reference speed) of the drive system. The non-linearity due to saturation in the magnetic circuit of the motor is also considered in the dynamic model. The basic equation of the induction was taken from reference [2].

2.4. Inverter model. The inverter operates on the principle of current control, wherein the inverter establishes currents (i_{as} , i_{bs} and i_{cs}) through the motor windings which tracks the reference currents (i_{as}^* , i_{bs}^* and i_{cs}^*).

A reference current being compared with the feedback current of the motor windings generates the ON/OFF signals for the switches in the IPM (Intelligent Power Module).

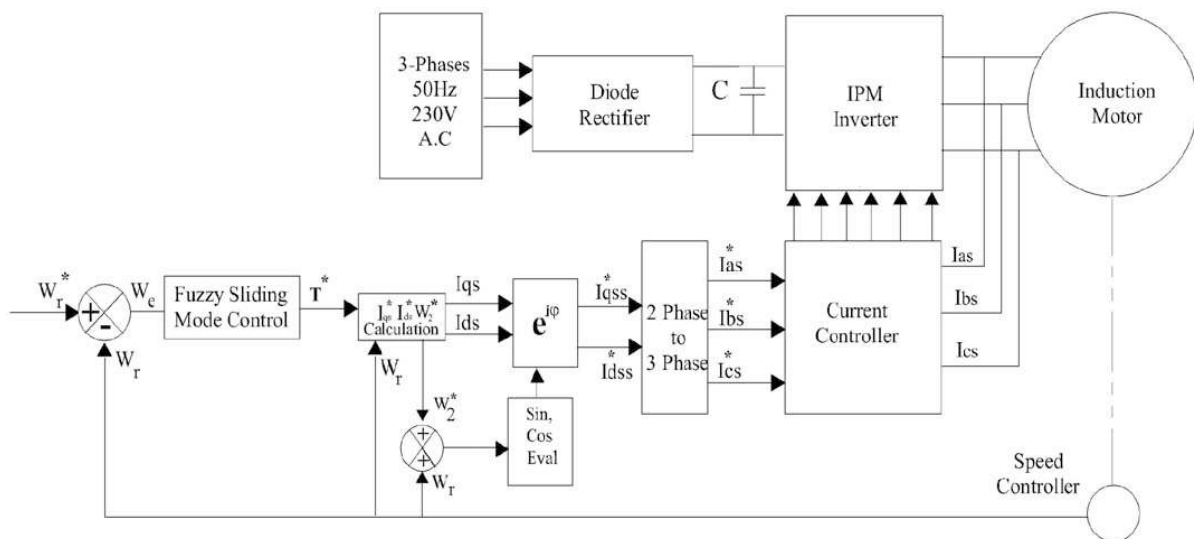


FIGURE 4. Block diagram of the proposed control scheme

3. Proposed Control Structure. The complete computation model of FSMC is shown in Figure 4. The reference speed W_r^* is compared with the actual rotor speed W_r to obtain the speed error, it is processed by the speed controller, which happens to be an SMC based on fuzzy logic (FL), and output of the controller is then used as reference torque (T^*). The speed controller responds quickly to changes in load, thereby improving the dynamic response. The torque reference T^* generates the flux component I_{qs}^* . A flux estimator present in the model uses W_r to obtain i_{mr}^* (the reference magnetizing current), and slip calculator evaluates i_{qs}^* and the reference slip W_2^* .

In this work the stationary reference frame model was selected as it is free from the system operating frequency and reduces computational burden. Rotor actual speed W_r^* and W_2^* are used to evaluate the flux angle δ . The angle δ is used to convert the field coordinate currents i_{ds}^* (torque producing component) and i_{qs}^* from the synchronous rotating reference frame to stationary frame. By using reverse park transformation i_{ds}^* and i_{qs}^* are converted into i_{dss}^* and i_{qss}^* which is the two-phase reference current in the stationary reference frame.

The i_{dss}^* and i_{qss}^* are used to generate the three phase reference currents, being used by the current controller to supply the needed gate pulses for the IPM. The current vectors and associated angles are pictorially represented in Figure 5.

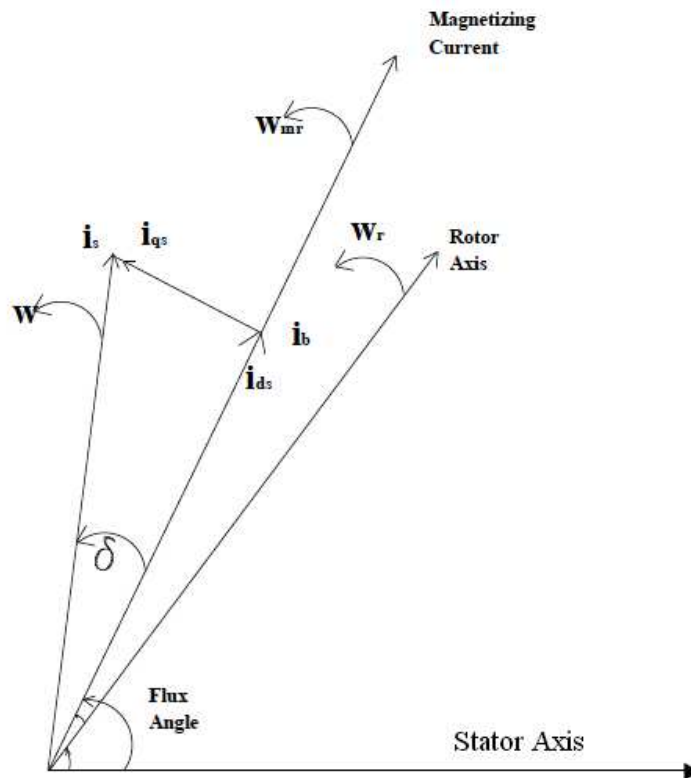


FIGURE 5. Current vectors

3.1. Fuzzy based sliding mode controller. Fuzzy logic and artificial neural network for stator flux and torque control has been investigated by researchers [22,23]; conceivably the hardware implementation on a low cost FPGA is not scrutinized. A fuzzy system generally comprises a fuzzification, fuzzy inference engine, fuzzy rule base and defuzzification. The addition of fuzzy logic to sliding mode control provides a robust controller with acceptable performance over a wide range of uncertainties and brings about reduction in chattering, without sacrificing the system performance.

The sliding mode control approach uses a sliding surface to model the desired closed-loop performance in state variable space. The controller forces the state trajectories into the sliding surface, where the values of switching functions $Y_{1(n)}$ and $Y_{2(n)}$ at the n^{th} sampling instants are as follows:

$$\begin{aligned} Y_{1(n)} &= +1, \text{ if } zx_{1(n)} \geq 0 \\ &= -1, \text{ if } zx_{1(n)} < 0 \\ Y_{2(n)} &= +1, \text{ if } zx_{2(n)} \geq 0 \\ &= -1, \text{ if } zx_{2(n)} < 0 \end{aligned}$$

where, $x_{1(n)}$ = speed error at the n^{th} sampling instant = $W_{r(n)} - W_r^*$, $x_{2(n)} = \dot{x}_{1(n)}$ = derivative of speed error $x_{1(n)}$ and z = switching hyper plane = $kx_{1(n)} + x_{2(n)}$.

The output of the variable structure controller $T_{(n)}$ is given by,

$$T_{(n)} = P_1 x_{1(n)} y_{1(n)} + P_2 x_{2(n)} y_{2(n)}$$

where k , is an adjustable parameter and P_1 and P_2 are fuzzy based controller gains. The FSMC has replaced the convention PI based speed controller.

3.2. Fuzzification. The fuzzy logic has emerged as a steering for machines, in complex industrial applications, as well as household and entertainment electronics. The first step in implementation of a fuzzy system is the declaration of input and output variables. Two input variables error and change in error were used with torque demand as the output (obtained from P_1 and P_2). The variables for input and output were all normalized in the region 0 to 1. Fuzzification refers to the process of converting the crisp variables into fuzzy variables. The variables for each input function were represented by triangular membership function with linguistic variables NB (Negative Big), NM (Negative Medium), NS (Negative Small), Z (Zero), PS (Positive Small), PM (Positive Medium) and PB (Positive Big), as shown in Figure 6(a).

3.3. Fuzzy inference and rule base. The fuzzy knowledge system includes the data base and rule base. The data provides the information which is used to define the rule base. The rules take the form as in this example.

If Error is NL and Change in Error is NL Then T is NL

where, T represents the torque reference. In the proposed model 49 rules were defined, to execute the Mamdani inference mechanism (Figure 6(b)).

3.4. Defuzzification. In defuzzification the fuzzy variables are converted into crisp variables. The centre of gravity method was selected for defuzzification. The outputs from this block are P_1 and P_2 which are used to evaluate the reference torque (T).

4. Results and Discussions.

4.1. HIL implementation of FSMC. Research has shown that FPGA with signal processing features could be an appropriate alternative over DSP and analog solutions for low cost drives. Figure 7 shows the hardware setup based on an FPGA, to validate the proposed control scheme. The BASYS 2 a low cost FPGA chip was used as the slave controller, for the MATLAB based real time PC issuing control signals. The FPGA was programmed using impact software from Xilinx.

The fuzzy inference engine present in MATLAB was made to work on a PC powered by an i3 processor and communication with this unit was made through serial communication interface. The FPGA Xilinx Spartan 3-E FPGA features 100K gates, 18-bit multipliers, 72Kbits of fast dual-port block RAM, and 500MHz+ operation. The communication features available on this device are two full-speed USB port for FPGA configuration and

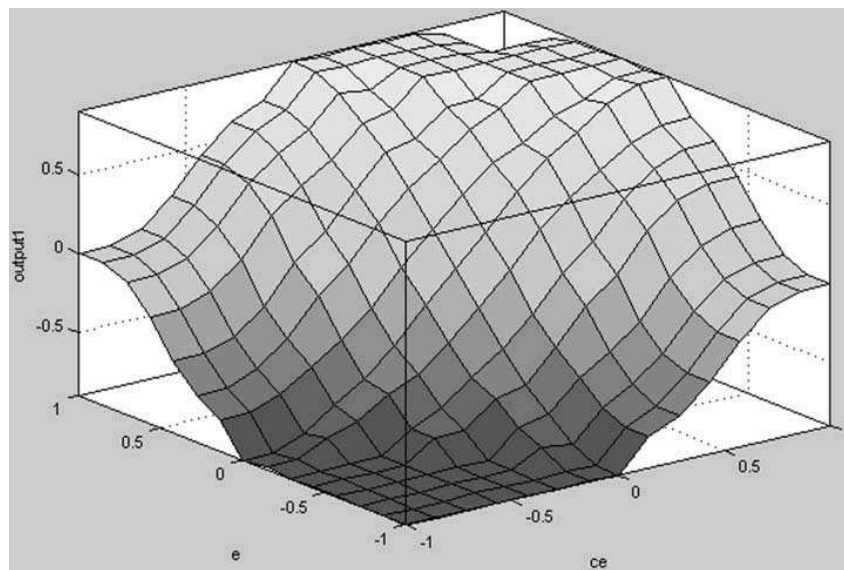
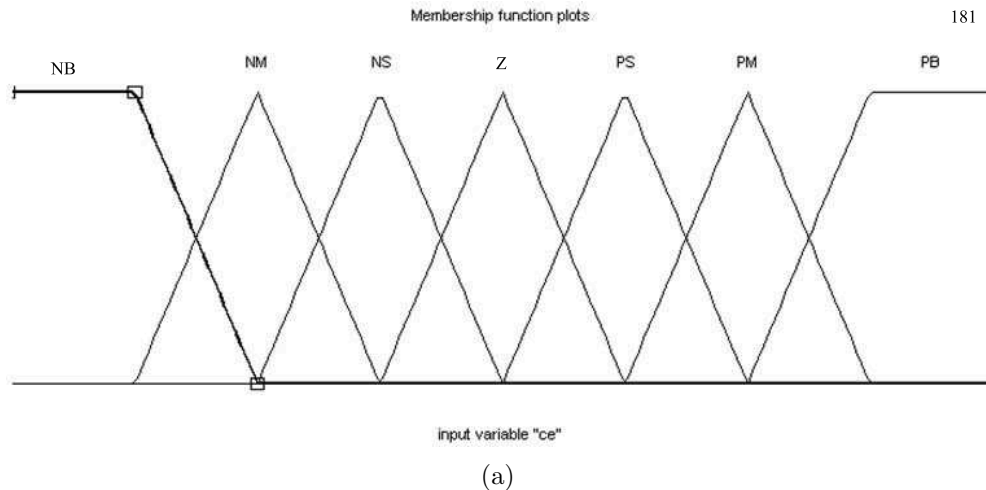


FIGURE 6. Fuzzy implementation, (a) input membership function error, (b) rule base of FSMC

data transfers (using Adept 2.0 – open source software). Three phase supply is rectified by using the Diode Rectifier module and the DC ripples are filtered by using an electrolytic capacitor. The inverter module uses this D.C supply as the power source. A 12-bit analog to digital converter card was used to read the speed information from the speed sensors and currents from the hall sensors.

The LOW power BASYS 2 processor when combined with the HIL features of MATLAB makes it suitable for applications in power control, lighting and alternate energy. It is notable that HIL feature was added to this device by means of a serial communication interface. The IPM used was INFINEON – BSM10GD120DN2 – IGBT MODULE, 1200V, ECONOPACK3 and aluminum heat sink was mounted on the device to reduce overheating under continuous operation. The IGBT driver form POWEREX VLM-504 was able to drive the IPM with +15 ON-State and –15V OFF-State voltages. IC provided two types of protection, one for over current and the other for under voltages, and a fault condition results in shutdown of all gate pulses and issue of fault signal to the P.C. The addition of Dead Band to the Gate pulses was done by means of the FPGA Verilog Code.

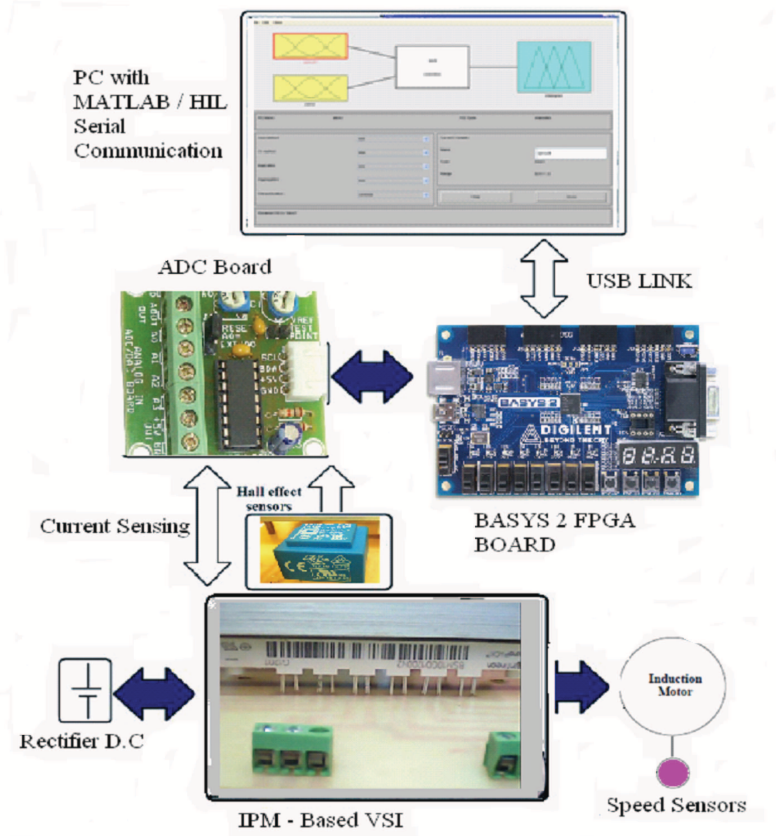


FIGURE 7. Hardware implementation of FSMC

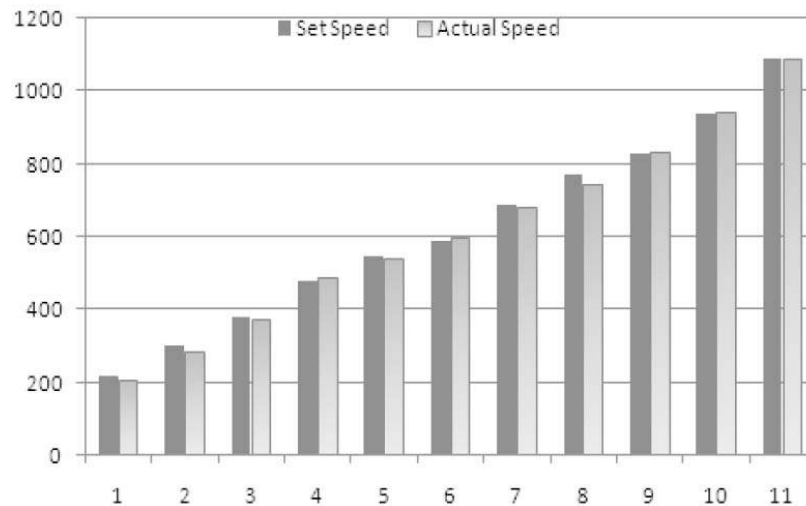


FIGURE 8. Experimental results for speed control

The ratings of the machine used for prototype testing are given in Table 2 (Appendix) and results compared for tracking with different reference speed scenarios are displayed in Figure 8. Machine parameters selected for the evaluation are given in Appendix-A Table 1. The drive was also subjected to load disturbance to test the robustness of the fuzzy sliding mode controller, and the same is discussed below.

4.2. Case 1 – starting performance. When three phase supply was fed directly to the machine, it runs at a speed of 1450 RPM. In this investigation the principle of soft starting was applied in order to reduce the inrush currents. The reference speed was set at 1160 RPM with the maximum limit on the reference torque being set at 150 Nm. The speed of the machine reaches steady state at 30 ms and the torque reaches the set value at 40 ms. SMC action was to ensure that the overshoots are settled down as soon as the machine reaches the set speed. When the set speed is reached after $t = 0$, the electrical torque decreases and becomes negative to maintain the motor speed at 1160 RPM. With the proposed FSMC the starting current was only twice that of rated full load current (Figure 9). The no-load current of the machine was 4 amps after reaching steady state.

4.3. Case 2 – speed reversal transients. In this experiment the speed reference was changed from +1140 RPM to -1140 RPM at time $t = 2$ seconds. In order to achieve this

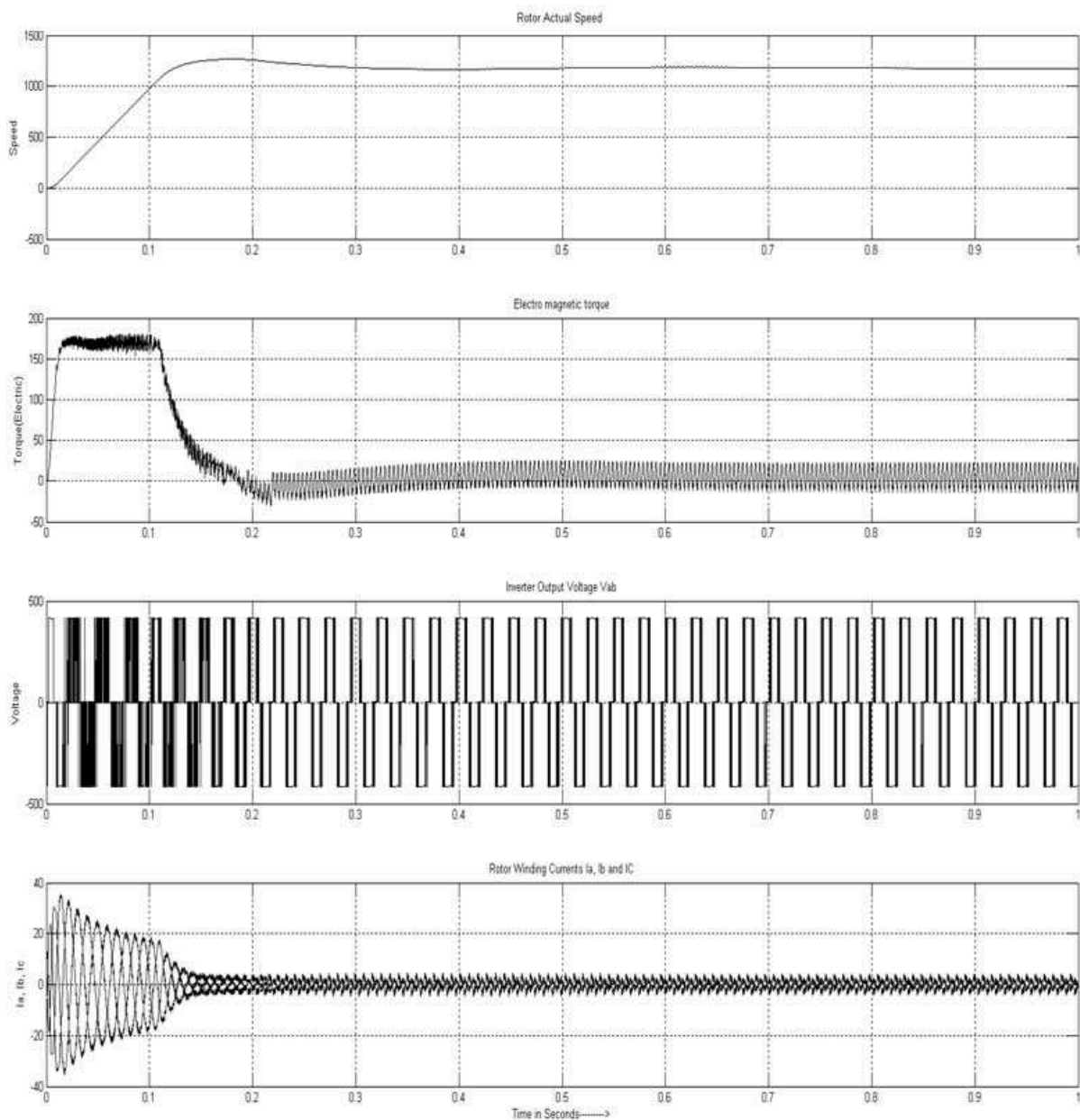


FIGURE 9. Starting current dynamics

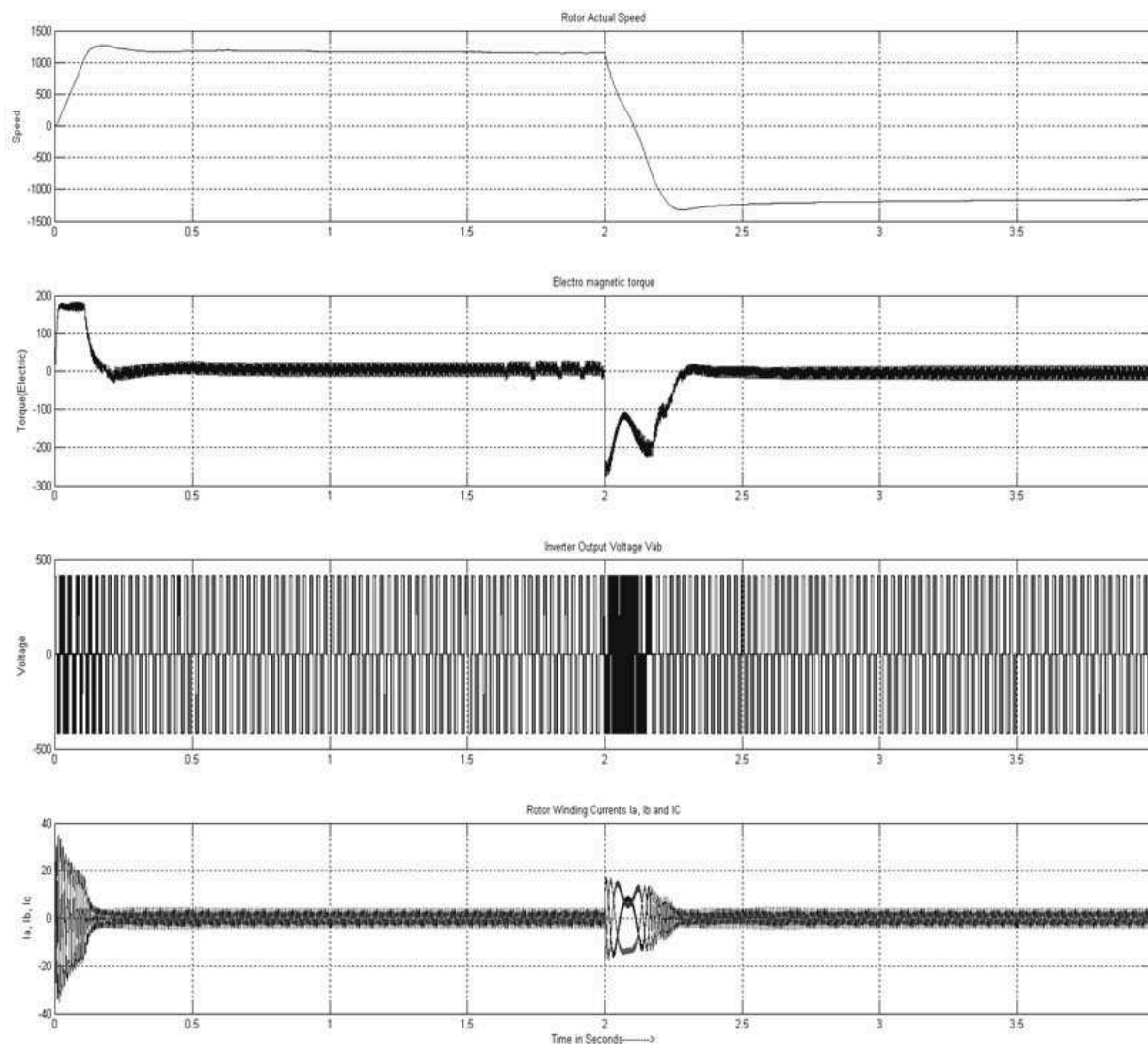


FIGURE 10. Speed reversal transients

speed reversal, the FSMC first reduces the frequency of the stator currents and then the three phase sequence was reversed at controlled frequency (Figure 10). The time taken to achieve the steady state in the reverse direction was 0.50 seconds after the issue of reversal command.

4.4. Case 3 – load perturbations. In this study a sudden load of 100N-M was applied at $t = 2$ seconds (i.e., after the machine has reached steady state). As displayed in Figure 11 load current shoots up-to 7A and reaches steady state of 6A after time duration of 0.01 seconds. When the load is removed at $t = 4$ seconds, there is an overshoot of 50 RPM in the rotor speed. This causes the speed controller output T to become negative and in addition the electromagnetic torque demand is made negative, and the speed starts to decrease. The machine attains steady state after 1 second. From this study it can be concluded that the machine remains stable to different load changes.

The delay timing for the protection circuit was adjusted to be 10 micro seconds. Inverter IPM is very sensitive to surges due to sudden loads and the IGBT gate pulses are to be disabled during spike currents (due to the de-saturation detection circuit); therefore, a smooth transition was created by tuning the membership function by trial and

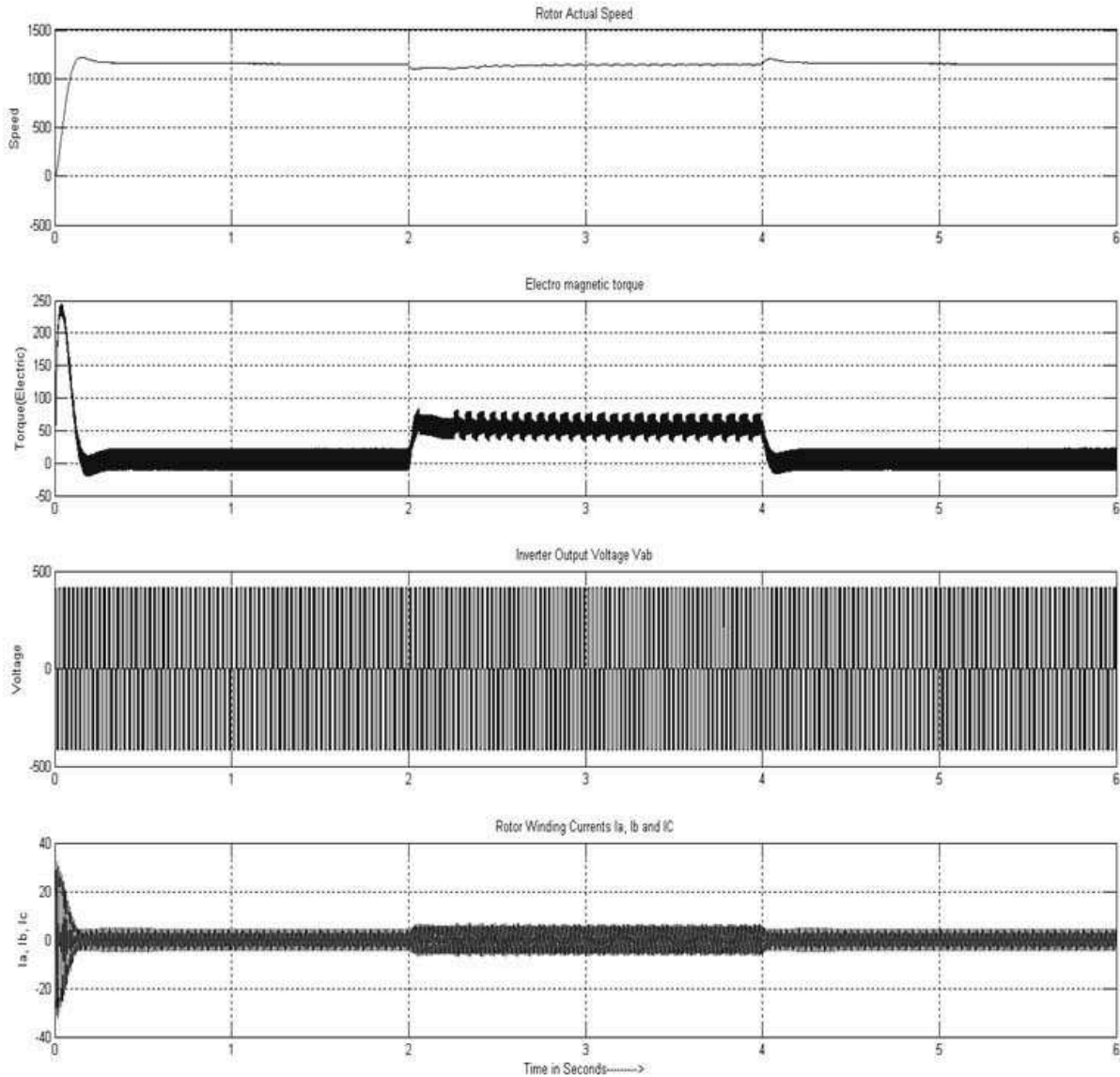


FIGURE 11. Load change scenarios

error process. This also ensures that the FSMC provides quicker response with reduced overshoot.

4.5. Robustness test. The robustness test was performed with variation of resistances and inductances of stator and rotor (as given in Table 1). This would represent the practical situation of overheating due to continuous operation under hot climatic conditions. The loading sequence similar to that of case 3 was applied. From the simulation results given in Figure 12 it can be observed that the speed remains unaffected by changing the parameters of Induction motor.

5. Conclusions. The detailed analysis of IM with fuzzy sliding mode speed controller confirmed that the proposed method provides a linear control, with a better dynamic response. This investigation has shown a fast change in the stator currents with change in reference speed or increase in mechanical load. Further, the parameter variation does not affect the performances of the proposed control method. The flux tracks the desired flux and it was insensitive to external, internal parameter variations of the machine. The

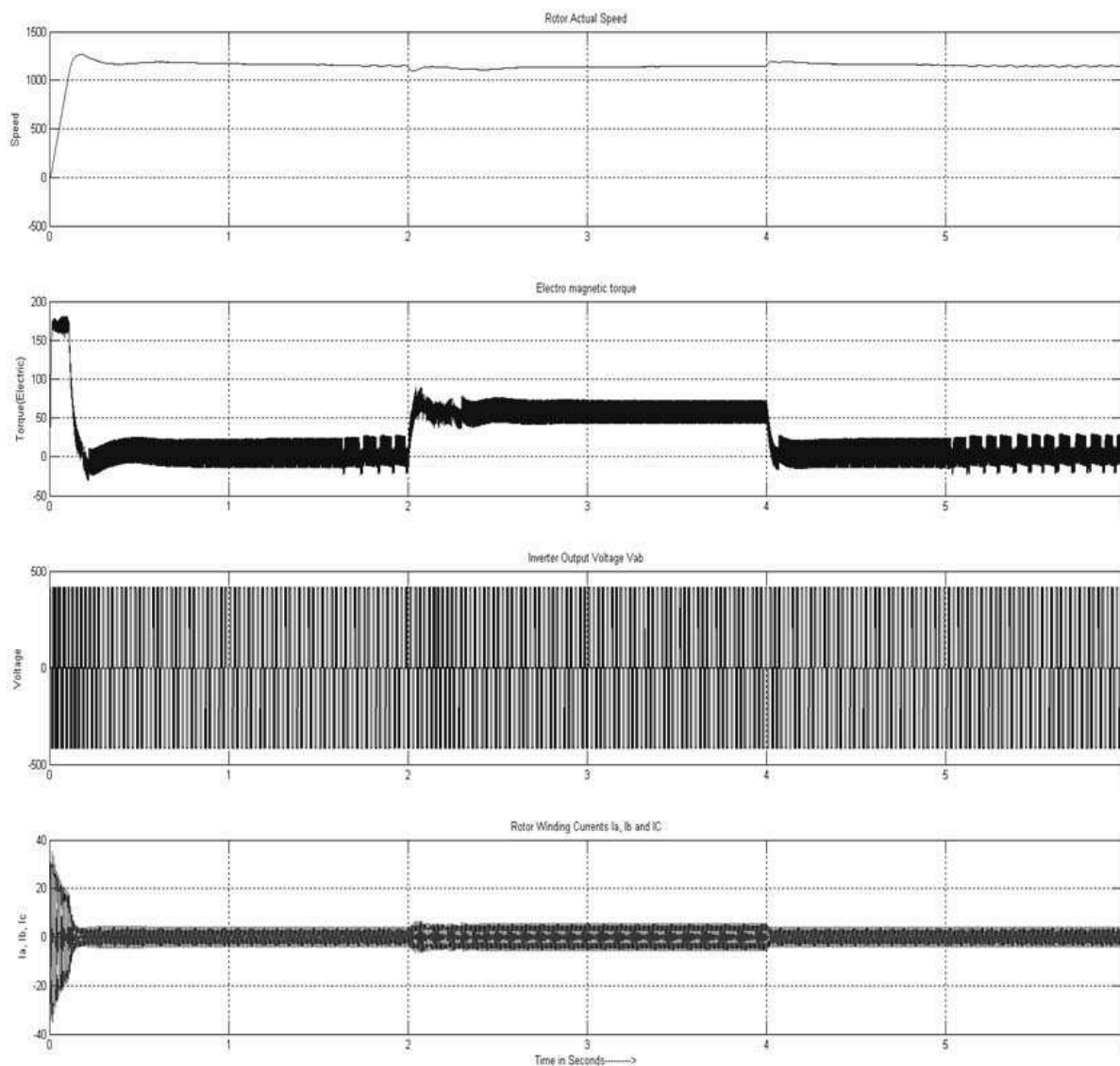


FIGURE 12. Simulations with parameter variation

decoupling between the flux and torque was maintained and starting current (torque) was limited drive by use of soft start method. The switching frequency of the design was 10 KHz which is well below the capability of the IPM. The design based on FPGA due to its low cost and robust nature makes it suitable for various industrial drive applications like process industries, textile mills, machine tools, lifts and traction systems.

REFERENCES

- [1] P. C. Sen, *Power Electronics*, 5th Edition, Tata MC-Graw Hill Publishing Company Limited, 2000.
- [2] B. K. Bose, *Modern Power Electronics and AC Drives*, 1st Edition, Pearson Education, Prentice Hall, 2001.
- [3] W. Leonhard, *Control of Electrical Drives*, Springer, 1996.
- [4] C. M. Ong, *Dynamic Simulation of Electrical Machinery*, Prentice Hall, NJ, 1989.
- [5] G. R. Slemon, *Electric Machines and Drives*, Reading, Addison-Wesley, MA, 1992.
- [6] S. E. Lyshevshi, *Electromechanical Systems, Electric Machines and Applied Mechatronics*, CRC Press, FL, 1999.
- [7] S. K. Biswas, Vector decoupled control of current fed induction motor, *Journal of Inst. Eng.*, vol.72, pp.48-53, 1991.

- [8] E. Merabet, R. Abdessemed, H. Amimeur and F. Hamoudi, Field oriented control of a dual star induction machine using fuzzy regulators, *The 4th Int. Conf. Computer Integrated Manufacturing*, Algeria, 2007.
- [9] R. Bojoi, A. Tenconi, G. Griva and F. Profumo, Vector control of dual three-phase induction-motor drives two current sensors, *IEEE Trans. Industrial Applications*, vol.42, no.5, pp.1284-1292, 2006.
- [10] R. Bojoi, M. Lazzari, F. Profumo and A. Tenconi, Digital field-oriented control for dual three-phase induction motor drives, *IEEE Trans. Industrial Applications*, vol.39, no.3, pp.752-760, 2003.
- [11] G. K. Singh, K. Nam and S. K. Lim, A simple indirect field-oriented control scheme for multiphase induction machine, *IEEE Trans. Ind. Electron.*, vol.52, no.4, pp.1177-1184, 2005.
- [12] P. C. Krause, *Analysis of Electric Machinery*, McGraw-Hill, New York, 1986.
- [13] F. Blaschke, The principle of field orientation as applied to the new TRANSVEKTOR closed-loop control for rotating field machines, *Siemens Review*, pp.217-220, 1972.
- [14] M. Depenbrock, Direct self-control (DSC) of inverter-fed induction machine, *IEEE Trans. Power Electronics*, vol.3, pp.420-429, 1988.
- [15] E. El-Gendy et al., A sliding mode controller for a three phase induction motor, *International Journal of Computer Applications*, vol.64, no.11, 2013.
- [16] S. Sathikumar and J. Vithayathil, Digital simulation of field oriented control of induction motor of CSI-fed induction motor, *IEEE Trans. Industrial Electronics*, vol.31, pp.141-148, 1984.
- [17] E. Y. Y. Ho and P. C. Sen, Decoupling control of induction motor drives, *IEEE Trans. Industrial Electronics*, vol.35, pp.253-262, 1988.
- [18] V. I. Utkin, Variable structure systems with sliding modes, *IEEE Trans. Automation Control*, vol.22, no.2, pp.212-222, 1977.
- [19] S. J. Huang and H. Y. Chen, Adaptive sliding controller with self-tuning fuzzy compensation for vehicle suspension control, *Mechatronics*, vol.16, pp.607-622, 2006.
- [20] C. Lascu, I. Boldea and F. Blaabjerg, Direct torque control of sensorless induction motor drives: A sliding-mode approach, *IEEE Trans. Industry Applications*, vol.40, no.2, pp.582-590, 2004.
- [21] A. Derdiyok, M. Guven, H. Rehman, N. Inanc and L. Xu, Design and implementation of a new sliding-mode observer for speed sensorless control of induction machine, *IEEE Trans. Industrial Electronics*, vol.49, no.5, pp.1177-1182, 2002.
- [22] A. Mir, M. E. Elbuluk and D. S. Zinger, Fuzzy implementation of direct self control of induction motors, *IEEE Trans. Industrial Applications*, vol.22, no.5, pp.820-827, 1986.
- [23] P. Z. Grabowski, M. P. Kazmierkowski, B. K. Bose and F. Blaabjerg, A simple direct-torque Neuro-fuzzy control of PWM-inverter-fed induction motor drive, *IEEE Trans. Industrial Electronics*, vol.30, pp.729-735, 1994.

Appendix-A.

TABLE 1. Induction machine normal ratings

Parameter Name	Normal Values	For Robustness Test
Machine type	Squirrel Cage, Three phase, 50 Hz	Squirrel Cage, Three phase, 50 Hz
Power	30 HP	30 HP
Speed	1440 rpm	1440 rpm
Stator Resistance R_s	0.248 Ohms	0.31 Ohms
Rotor resistance R_r	0.25 Ohms	0.31 Ohms
Stator Reactance X_{Ls}	0.43 Ohms	0.537 Ohms
Rotor Reactance X_{Lr}	0.43 Ohms	0.537 Ohms
Number of Poles P	4	4
Mutual Inductance M	0.06	0.06
Moment of Inertia J	0.305 Kg-m ²	0.305 Kg-m ²

TABLE 2. IM used in prototype testing

Machine type	Squirrel Cage
Power	3 HP
Speed	1400 RPM
Ambient Temperature	45 Degree C
Pole	4
Supply	Three phase, 50 Hz, 415 V
Frame	56 NEMA